Nuclear Magnetic Resonance

Ethan Kasaba, Raymond Niu, Andre Barbosa
Rutgers University

In this experiment, we investigated the nuclear magnetic resonance (NMR) of light mineral oil, deionized water, and ethyl alcohol using a permanent magnet, pulse programmer, synthesizer, and amplifier-receiver. By analyzing the magnitude of the transverse magnetic field of each sample, we examined the magnetic resonance behavior near the resonance frequency of the proton. Experimental data from different pulse sequences were fitted to exponential decay models to extract the spin-lattice relaxation time T_1 and spin-spin decoherence time T_2. For mineral oil, we measured $T_1 = 49.79(20)$ ms and $T_2 = 41.0(6)$ ms; for deionized water $T_1 = 1.84(3)$ s and $T_2 = 691(16)$ ms; and for ethyl alcohol $T_1 = 1.351(18)$ s and $T_2 = 420(40)$ ms. Additionally, we estimated the magnetic field inhomogeneity of the permanent magnet as $\Delta B_0 = 4.1219(18)$ µT. We also qualitatively characterized the frequency drift of the system as a function of time, attributing it to the permanent magnet and electronic components not being in thermal equilibrium.

INTRODUCTION AND THEORY

Introduction

Nuclear Magnetic Resonance (NMR) is a technique that examines atomic nuclei in a magnetic field by applying a pulse of radiofrequency (RF) energy to excite the nuclei. Discovered by Felix Bloch and Edward Purcell in 1946, NMR reveals information about molecular structure and environment. Notably, its principles of spin manipulation have also laid foundational concepts for quantum computing. This experiment uses pulse NMR to observe proton behavior in light mineral oil, providing insights into its molecular properties.

Nuclear Magnetization

Magnetic resonance occurs in many stable nuclei due to their non-zero magnetic moment and angular momentum, which arise from their intrinsic spin nature. The magnetic moment $\boldsymbol{\mu}$ of a nucleus is related to the angular moment $\mathbf{J}$ and and the spin $\mathbf{I}$ in the following way:

$$\boldsymbol{\mu} = \gamma \mathbf{J} = \gamma \hbar \mathbf{I}$$

where $\hbar$ is the reduced Plank's constant and the proportionality factor γ is the gyromagnetic ratio unique to each kind of nuclei. When the nucleus is put under a magnetic field $\mathbf{B_0} = B_0 \hat{\mathbf{z}}$, the magnetic energy E associated with the magnetic moment is given by:

$$E = -\boldsymbol{\mu} \cdot \mathbf{B_0} = -\mu_z B_0 = -\gamma \hbar I_z B_0$$

In Quantum mechanics, I_z, the z component of the spin, is given the magnetic quantum number m_I of the nucleus as:

$$I_z = m_z = -I, -(I-1), ..., I-1, I$$

Specifically for both proton and fluorine nuclei, the spin $I = 1/2$, which means there are only two possible magnetic energy states with an energy separation ΔE given by:

$$\Delta E = \gamma \hbar B_0 = \hbar \omega_0$$

where the associated angular frequency $\omega_0 = \gamma B_0$ is called the Larmor frequency.

Consider a one-milliliter sample of mineral oil, containing N protons, placed under a constant magnetic field $\mathbf{B_0} = B_0 \hat{\mathbf{z}}$. When the thermal equilibrium is reached, the ratio of the number of protons in the lower energy state (N_2) and the higher energy state (N_1) is given by the Boltzmann factor as:

$$\frac{N_2}{N_1} = e^{\frac{\Delta E}{k_B T}} = e^{\frac{2\mu_z B_0}{k_B T}}$$

where k_B is the Boltzmann constant and T is the temperature. Then, the total magnetization M_0 at the equilibrium is given by:

$$M_0 = (N_1 - N_2)\mu_z = N\mu_z \, tanh(\frac{\mu_z B_0}{k_B T})$$

π Pulse and $\frac{\pi}{2}$ Pulse

So far, we have only considered applying a constant external magnetic field in the z-direction. When adding a circularly polarized (with an angular frequency of ω) magnetic field $\mathbf{B_1}(t)$ in the xy plane, the total magnetic field $\mathbf{B}(t)$ is then:

$$\begin{aligned}\mathbf{B}(t) &= \mathbf{B_1}(t) + \mathbf{B_0} \\ &= B_1 \cos(\omega t)\, \hat{\mathbf{x}} + B_1 \sin(\omega t)\, \hat{\mathbf{y}} + B_0 \hat{\mathbf{z}}\end{aligned}$$

To analyze this oscillating field, we work in a rotating frame, around the z axis, with an angular frequency ω, such that the magnetic field on the xy plane $\tilde{\mathbf{B}}_1(t) = B_1 \tilde{\mathbf{x}}$ is stationary in the x-direction. Along the z axis, the rotating coordinate system introduces an additional magnetic field correction term $\tilde{\mathbf{B}}_{\text{corr}} = -(\omega/\gamma)\tilde{\mathbf{z}}$, which

results in the total effective magnetic field in the rotating frame $\tilde{\mathbf{B}}_{\text{eff}}(t)$ given as:

$$\tilde{\mathbf{B}}_{\text{eff}}(t) = \tilde{\mathbf{B}}_{\text{eff}} = B_1\,\tilde{\mathbf{x}} + (B_0 - \frac{\omega}{\gamma})\,\tilde{\mathbf{z}}$$

Here, we consider a specific case where the external drive is on resonance with the Larmor frequency of the nucleus (i.e., $\omega = \omega_0 = \gamma\,B_0$). Then, the effective magnetic field $\tilde{\mathbf{B}}_{\text{eff}}(t) = B_1\,\tilde{\mathbf{x}}$ is a constant in the $\tilde{\text{x}}$-direction. In this case, Newton's second law gives the equation of motion of the magnetization $\tilde{\mathbf{M}}(t)$ as:

$$\frac{d\tilde{\mathbf{M}}(t)}{dt} = \gamma\,\tilde{\mathbf{M}}(t) \times \tilde{\mathbf{B}}_{\text{eff}} = \gamma B_1\,\tilde{\mathbf{M}}(t) \times \tilde{\mathbf{x}}$$

which describes a precessing motion of $\tilde{\mathbf{M}}(t)$ around the $\tilde{\text{x}}$ axis.

If we wait for the magnetization to reach the thermal equilibrium (i.e., $\tilde{\mathbf{M}}(0) = M_0\,\tilde{\mathbf{z}} = M_0\,\hat{\mathbf{z}}$) first, and then turn on the oscillating field, the magnetization $\tilde{\mathbf{M}}(t)$ would precess on the $\tilde{\text{y}}\tilde{\text{z}}$ plane with an angular frequency $\omega_1 = \gamma\,B_1$. This allows us to perform $\frac{\pi}{2}$ pulse and π pulse on the magnetization. To perform a $\frac{\pi}{2}$ pulse, we need to keep the rotating field on for only $t_{\frac{\pi}{2}} = \frac{\pi}{2\omega_1}$ before turning it off, then the magnetization will be brought onto the xy plane. For a π pulse, we set the the pulse time $t_\pi = \frac{\pi}{\omega_1}$, which completely flips the magnetization from $M_0\,\hat{\mathbf{z}}$ to $-M_0\,\hat{\mathbf{z}}$.

$\mathbf{T_1}$, $\mathbf{T_2}$, and $\mathbf{T_2^*}$ Relaxation Time

Back to the case when only $\mathbf{B_0} = B_0\,\hat{\mathbf{z}}$ is present, the magnetization M_0 does not happen instantaneously. Rather, the build-up of the magnetization $M_z(t)$ follows the differential equation:

$$\frac{dM_z(t)}{dt} = \frac{M_0 - M_z(t)}{T_1}$$

where T_1 is the characteristic time scale associated with the z component relaxation of the magnetization. If we solve this differential equation and set the initial magnetization to be $-M_0$, the solution is given as:

$$M_z(t) = M_0\,(1 - 2e^{-\frac{t}{T_1}}) \tag{1}$$

The magnetization crosses zero at $t = \tau_0$, which is related to T_1 as:

$$T_1 = \frac{\tau_0}{\ln 2} \tag{2}$$

During the magnetization process, the spin system goes to a lower energy state, and releases energy to the surroundings, which are referred to as "the lattice." Therefore, T_1 is called the spin-lattice relaxation time.

Now, in the case when a $\frac{\pi}{2}$ pulse is applied to a thermal equilibrium state, the magnetization in the transverse plane also decays while precessing around the magnetic field in the z-direction. In the lab frame, the decay satisfies the following differential equations:

$$\frac{dM_{xy}(t)}{dt} = \frac{M_{xy}(t)}{T_2}$$

where T_2 is the spin-spin relaxation time and $M_{xy}(t)$ is the magnitude of the magnetization on the xy plane. With the initial condition of $M_{xy}(0) = M_0$, the solution becomes:

$$M_{xy}(t) = M_0\,e^{-\frac{t}{T_2}} \tag{3}$$

The spin-spin relaxation happens due to the magnetic fields generated by neighboring nuclei, causing the precession of each nuclei to have slightly different frequencies, and thus leads to the dephasing of the magnetization.

In the T_2 discussion above, we treat the magnetic field to be uniform over the sample. However, in most cases, including our experiment setup, the magnetic field $\mathbf{B_0}$ varies in location, and the inhomogeneity of the field ΔB_0 also causes the nuclei to precess at different frequencies. Accounting for this source of magnetization relaxation in the transverse plane, the characteristic time T_2^* of the decay in $M_{xy}(t)$, so-called Free Induction decay (FID), is given as:

$$\frac{1}{T_2^*} = \frac{1}{T_2} + \gamma\,\Delta B \tag{4}$$

Self-Diffusion

Self-diffusion is the process in which a magnetic field gradient causes an alteration in the phase of the magnetic moments in the material, causing spin-spin decoherence, affecting the measured T_2. This self-diffusion causes the spins to dephase faster than an accurate T_2 would suggest. For the case where the magnetic field gradient, $\partial B/\partial z$, is in the z-direction, the effect of self-diffusion can be characterized by an extra cubic term in the exponent of the spin-spin relaxation function:

$$M_{xy}(t) = M_0\,e^{-(\frac{t}{T_2} + \frac{Kt^3}{n^2})} \tag{5}$$

where n is the number of π-pulses used to measure $M_{xy}(t)$ and constant the K is given as:

$$K = -\gamma^2(\frac{\partial B}{\partial z})\frac{D}{12} \tag{6}$$

where D is the diffusion constant.

APPARATUS AND PROCEDURE

Our primary apparatus for this experiment was the Teach-Spin PSA-2 device. This apparatus is comprised of four separate modules, of which we used three. The fourth module is for continuous-wave NMR, which is outside the scope of the experiment. To see the precession, a permanent magnet with a field strength of 0.5T was utilized. Within this magnetic field is a coil that is used to send the pulses to the sample as well as to pick up the resonant response. To make the magnetic field as homogeneous as possible, a PS2 controller enables fine tuning of the magnet temperature and magnetic field gradient. Finally, our readout was done on a Keysight EDUX1052A oscilloscope, with a 1 Gigasample per second sampling rate.

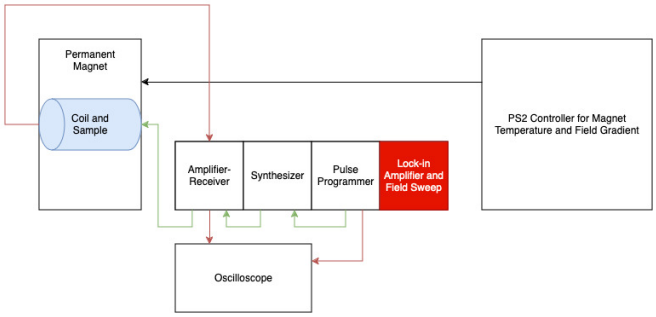

FIG. 1: Experimental Setup

The pulse process begins in the pulse programmer, where the desired pulse times are inputted. The pulse programmer is capable of outputting 1 A pulse and up to 100 B pulses. The A and B pulses are separated by a controllable time τ, and the time between B pulses is 2τ. The final variable in the pulse programmer is the period between pulse sequences, which can be adjusted to ensure the spins in the sample properly return to equilibrium before initiating the next sequence of pulses.

Components of the Teach-Spin Device

The pulse programmer then communicates with the 21 MHz synthesizer, which synthesizes the pulses into the proper frequency sinusoidal wave for the chosen amount of time. This synthesizer can synthesize waveforms of over 30MHz, but this frequency is extraneous for our experiment. Here, the resonant frequency of the sample is inputted, which for our sample of light mineral oil is about the resonant frequency of the proton for our field strength, which depending on the temperature of the magnet, averaged about 21.9MHz. Additionally, other variables can be changed such as the global phase, and continuous wave variables, but these were unneeded for our experiment.

The pulses are then sent into the receiver, which are forwarded into the coil to affect the sample. The response from the sample is then sent into the same coil which is sent back to the receiver. In the receiver, the response goes through a low-noise amplifier that amplifies the signal by 20dB. The signal then goes through a variable gain amplifier, which can vary from 0-80dB, but for our experiment was set to approximately 65dB. Following this, the response goes through a band-pass filter that only allows either proton or flourine resonant frequencies through, which was set to the proton band for our experiment. Finally, the incoming signal is sent through a rectifier, before the response envelope is sent to the oscilloscope for readout. The trigger for the oscilloscope is set from the pulse programmer, which sends a trigger pulse to accurately trigger at the proper time to capture the envelope. The data from the oscilloscope was downloaded onto a computer for analysis in a Jupyter notebook.

Choosing Pulse Parameters

To conduct material characterization, first the resonance frequency must be known. To get the resonance frequency, we can send in a sweep of frequencies to the sample, and examine the "I OUT" from the receiver, which is the product of the response from the sample and the waveform from the synthesizer. By choosing our pulse frequency such that the beating seen in this output is minimized, we can ensure that our pulses are sent at the correct resonant frequency for the material and field strength. Optimizing in this way works because the beating frequency is directly determined by the difference between the pulse frequency and the resonance frequency of the material. Thus, by minimizing this beating frequency, we get as close to the Larmor frequency as within our equipment's capability, which is within 10Hz, as determined by the synthesizer.

After determining the resonance frequency, the proper pulse times for two types of pulses must be determined so that the necessary pulse sequences are possible. First is the π pulse, which rotates the magnetization of the spins from alignment in the $\hat{z}$ direction, to alignment in the $-\hat{z}$ direction, which is a rotation by 180° or π rotation. This pulse time can be determined from varying the pulse time until the FID signal is minimized. The FID signal specifically measures the magnitude of the magnetization in the x-y plane as function of spin-spin decoherence and decay from local field inhomogeneities. We typically measure it by aligning the spins in the x-y plane along an axis and letting them process and decohere over time. This procession that occurs during the decoherence of the spins is measured through the coil, yielding our FID signal. Since the FID signal only reads the magnitude of the magnetization in the x-y plane, by minimizing the FID signal amplitude, the π pulse time

can be accurately determined, since minimizing the x-y procession and thus FID signal amplitude means that all the spins must be aligned on the z-axis.

The second pulse time to obtain is the $\frac{\pi}{2}$ pulse time, which rotates the spins from alignment in the $\hat{z}$ direction, to being aligned in the x-y plane. This time can be found in one of two ways. First, and most simply, is to take the π pulse time and divide it by two, yielding the $\frac{\pi}{2}$ pulse time. Alternatively, the pulse time can be adjusted to maximize the FID signal, which is when all of the spins are aligned in the x-y plane. For our experiment, we divided the π pulse time by two, and checked to ensure it maximized the FID signal accordingly.

Pulse Sequences and Decay Constants

To characterize the materials, three decay constants must be known. First is T_2^*, the rate of decay of the FID signal. This decay constant is heavily impacted by magnetic field inhomogeneity, and thus is not critical in characterization, but is useful to know in any case. Second is T_1, the rate of spin-lattice relaxation. Third is T_2, the spin-spin relaxation time. By learning these three constants, a material is then characterized by through knowledge of its decay profile.

T_2^* can be determined from a simple one-pulse sequence, as shown in Figure 2. By applying a $\frac{\pi}{2}$ pulse, the spins are aligned into the x-y plane and the emit an FID signal. By capturing this signal on the oscilloscope and fitting it to an exponential curve, we can extract the exponential decay constant from the fit, yielding T_2^*. This is typically the fastest of the decay constants, since as previously stated, it is heavily reduced by field inhomogeneity.

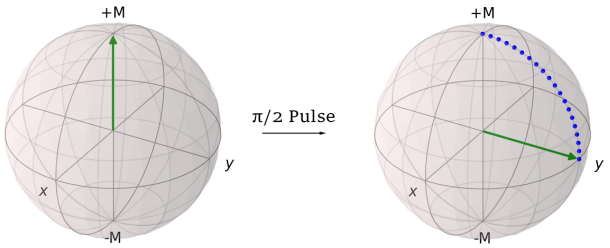

FIG. 2: The one-pulse sequence to measure the Free Induction Decay, a single $\frac{\pi}{2}$ pulse

The determination of T_1 can be done through a two-pulse sequence, visualized in Figure 3. First, a π pulse is applied to flip the magnetization. Then, after waiting some time τ, a $\frac{\pi}{2}$ pulse is applied. This "interrogates" the magnitude of the $\hat{z}$ magnetization, which otherwise cannot be directly measured. By varying τ and recording the amplitude following the $\frac{\pi}{2}$ pulse, data points of an exponential decay can be obtained, fitted, and then the decay constant extracted, to yield the spin-lattice relaxation time.

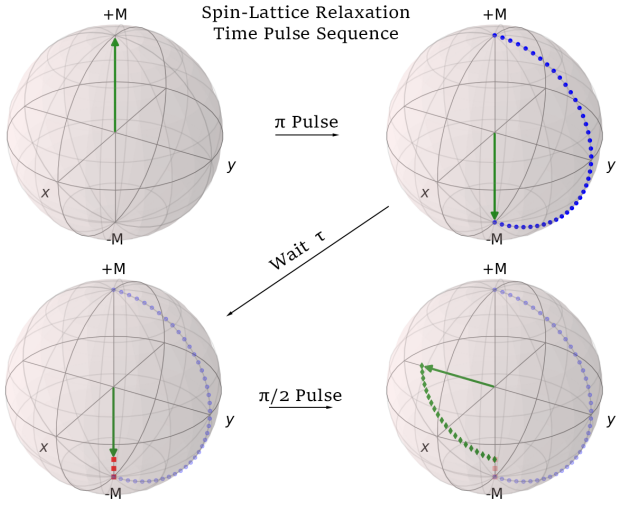

FIG. 3: The two-pulse sequence to measure T_1, one π pulse, waiting some time τ, and a $\frac{\pi}{2}$ pulse

The spin-spin relaxation time can be obtained in many ways, of which three are applicable to our experiment. The simplest is through the two-pulse spin-echo sequence, shown in Figure 4. First, a $\frac{\pi}{2}$ is sent to the sample, and the spins begin to process at slightly differing rates due to local field inhomogeneities. After waiting some time τ, a π pulse is then applied. Then, after waiting for another τ, the so-called "echo" amplitude can be seen. Similar to the T_1 sequence, determining the echo amplitude as a function of τ and extracting the decay constant yields T_2. This is because the echo amplitudes decay only due to spin-spin decoherence, and are unaffected by spin-lattice decay. Thus, fitting the echo amplitude as a function of τ to an exponential decay function, which matches theory, the decay constant of the fit is the T_2 time.

The spin-echo pulse sequence, while efficient due to only requiring two pulses, is subject to self-diffusion within the material, accelerating the decay rate as τ becomes longer. To combat this, a more sophisticated pulse sequence, known as the Carr-Purcell sequence, can be used. This sequence uses a series of π pulses after the initial $\frac{\pi}{2}$ pulse, each separated by a time 2τ. This helps minimize the self-diffusion within the material. By picking a large amount of π pulses, and fitting the peaks from the corresponding echo amplitudes from each of these pulses to an exponential decay, a more accurate T_2 time can be determined.

However, there is one problem with the Carr-Purcell sequence. If the π pulse time is not exactly right, the slight error from each pulse will compound resulting in erroneous data after the first few π pulses. This is noticeable in the response from the sample due to the often

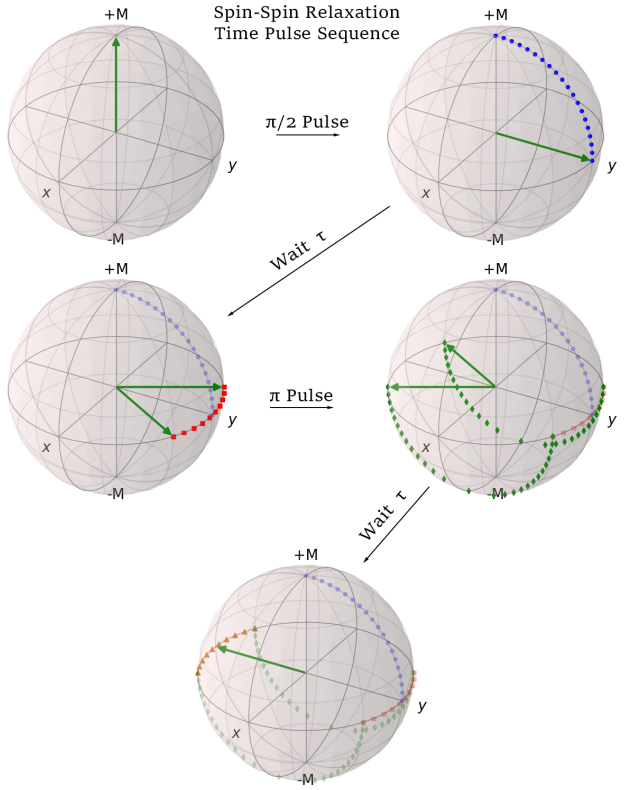

FIG. 4: The two-pulse sequence to measure T_2, one $\frac{\pi}{2}$ pulse, waiting some time τ, a π pulse, and waiting another τ

seen beating behavior in the echo amplitudes, as shown in Figure 5. This beating occurs due to how the accumulated error affects the magnetization. After many π pulses, the accumulated error results in the magnetization being almost completely z-polarized. The error than continues to accumulate and bring the net magnetization back to the x-y plane, where the apex of the "beat" is seen. This cycle then repeats for the duration of the pulse sequence.

To combat this error accumulation from even the smallest of errors after many pulses, the Meiboom-Gill pulse sequence eliminates the accumulation of error through applying subsequent π pulses rotated 90° to the plane of the initial excitation pulse, which mitigates cumulative errors from occurring. This is the most accurate way to determine T_2 since it accounts for both self-diffusion and cumulative phase errors from successive pulses.

Finally, through comparing the T_2 times obtained from the spin-echo sequence and the Meiboom-Gill sequence, the effect of self-diffusion on the system can be ascertained, to see if it has a non-negligible impact on the decay when measuring using the spin-echo pulse sequence.

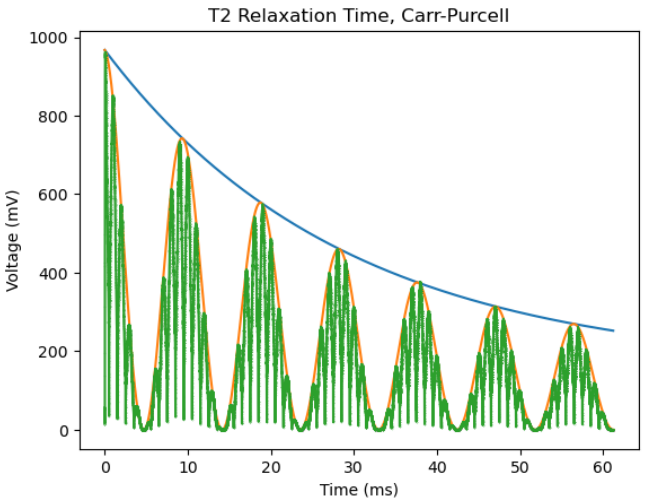

FIG. 5: Theoretical simulation of the beating behavior seen in the Carr-Purcell sequence with 60 π pulses.

DATA AND ANALYSIS

We conducted a series of nuclear magnetic resonance (NMR) experiments using the TeachSpin PS2 NMR Spectrometer to characterize the transverse relaxation times T_2^* and T_2, as well as the longitudinal relaxation time T_1, for light mineral oil, deionized water, and ethyl alcohol. Additionally, we estimated the magnetic field inhomogeneity ΔB_0 of the system and assessed the impact of frequency drift during manual data acquisition. The results are summarized in Figures 6–10 and Tables I–II.

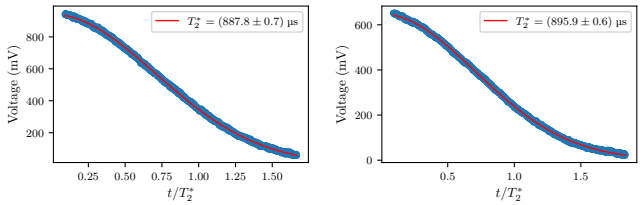

(a) Mineral Oil

(b) DI Water

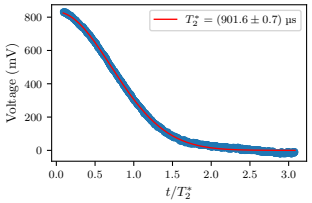

(c) Ethyl Alcohol

FIG. 6: Free Induction Decay.

Figure 6 shows the free induction decay (FID) following a $\pi/2$-pulse, where the induced voltage was recorded as a function of time. The data (error bars omitted

for errors smaller than marker size) were fit to a Gaussian: $V(t) = a\exp[-(t/T_2^*)^2] + b$, where a is the signal amplitude, b accounts for background noise and instrument calibration, and T_2^* characterizes the decay time. We observed nearly identical T_2^* across samples: $T_2^* = 887.8(7)\,\mu$s for mineral oil, $T_2^* = 895.9(6)\,\mu$s for deionized water, and $T_2^* = 901.6(7)\,\mu$s for ethyl alcohol. Although the ideal FID model is given by (3), a Gaussian provided a better fit due to magnetic field inhomogeneities causing spins to follow a normal distribution.

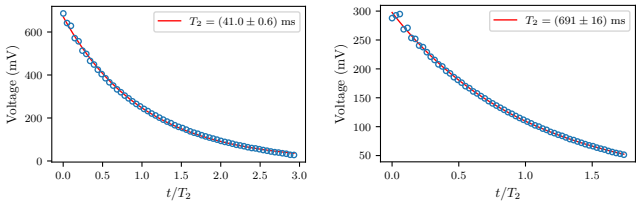

(a) Mineral Oil **(b)** DI Water

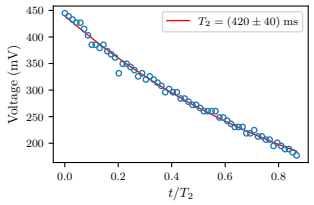

(c) Ethyl Alcohol

FIG. 7: Meiboom-Gill multipulse spin-echo sequence results.

Figure 7 depicts the transverse relaxation times T_2 measured using the Meiboom-Gill (M-G) multipulse spin-echo sequence. Spin-echo peak voltages were recorded over time and fit to: $V(t) = a\exp(-t/T_2) + b$. The results showed significant variation in T_2 among the samples, with the longest relaxation time observed for deionized water $T_2 = 691(16)$ ms, followed by ethyl alcohol $T_2 = 420(40)$ ms and mineral oil $T_2 = 41.0(6)$ ms. These differences reflect varying viscosities and molecular interaction rates, with deionized water exhibiting the least interactions and mineral oil the most.

Figure 8 shows the T_1 values obtained via an inversion-recovery method using a π-pulse followed by a $\pi/2$-pulse after a variable delay. Data were fit to: $V(t) = a[1 - 2\exp(-t/T_1)]$. Results indicate the longest T_1 for deionized water $T_1 = 1.84(3)$ s, followed by ethyl alcohol $T_1 = 1.351(18)$ s and mineral oil $T_1 = 49.79(20)$ ms. Water's relatively simple molecular structure minimizes energy dissipation, leading to a longer T_1.

Table I confirms T_1 values obtained using the zero-crossing method, which agree within one standard error with fits in Figure 8, bolstering confidence in our estimates of the longitudinal relaxation time.

Figure 9 explores T_2 using a single two-pulse spin-

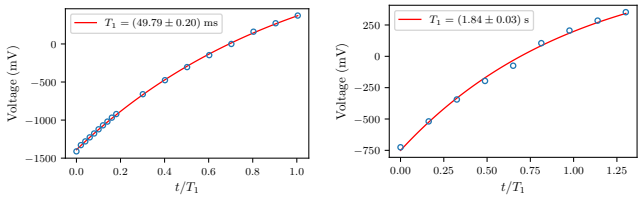

(a) Mineral Oil **(b)** DI Water

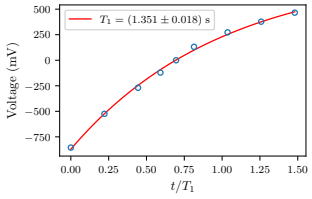

(c) Ethyl Alcohol

FIG. 8: Longitudinal relaxation times.

TABLE I: Longitudinal relaxation time calculated using the zero-crossing method.

Sample	T_1 (s)
Mineral Oil :	0.0487(12)
DI Water :	1.95(22)
Ethyl Alcohol :	1.363(7)

echo sequence ($\pi/2$-pulse followed by π-pulse after variable delay time). Echo heights were fit to: $V(t) = a\exp[-t/T_2 - Kt^3/n^2] + b$, where K given by (6) accounts for diffusion and $n = 1$ (one π-pulse). For deionized water, this method yielded a significantly shorter $T_2 = 235(17)$ ms compared to the M-G sequence. The single two-pulse sequence, conducted manually, is more susceptible to frequency drift due to the longer duration of data collection, especially for water, which requires larger time intervals between successive $\pi/2$-pulses due to its longer T_1.

Using the relationship: $\gamma\Delta B_0 = 1/T_2^* - 1/T_2 - 1/T_1$, we estimated ΔB_0 for each sample. Table II summarizes these results, showing consistent ΔB_0 values across

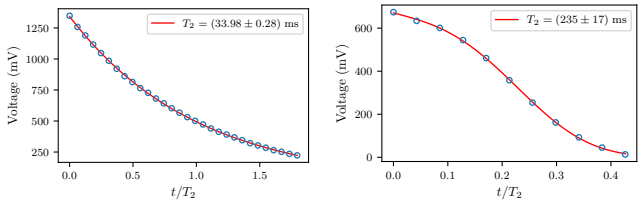

(a) Mineral Oil **(b)** DI Water

FIG. 9: Single two-pulse spin-echo results.

samples, as expected since ΔB_0 reflects properties of the permanent magnet rather than the samples. This is also consistent with the results of Figure 6, namely, $1/T_2^* \sim \gamma \Delta B_0$.

TABLE II: Calculated magnetic field inhomogeneity.

Sample	ΔB (μT)
Mineral Oil :	4.044(3)
DI Water :	4.1650(27)
Ethyl Alcohol :	4.134(4)

Figure 10 shows the frequency drift as a function of time for two different samples on two different days. The temperature in the lab fluctuates and so more data would need to be taken to draw definitive conclusions. However, the figure gives us an estimate and some intuition regarding how much the frequency drifts by during the course of our measurements. Based on the data which we fit to: $\Delta\nu(t) = \nu(t) - \nu_0 = (\nu_{\text{eq}} - \nu_0)\tanh(t/\tau)$, where ν_0 is the initial frequency set upon powering on the spectrometer and calibrating the system and ν_{eq} is the equilibrium frequency in the limit $t \to \infty$, we argue that it is best to wait some time allowing the system to equilibrate before performing measurements. Based on the data we estimate an approximate wait time of $\sim$ 20min for more stable data collection.

CONCLUSION

This report documents a comprehensive investigation of nuclear magnetic resonance (NMR) properties for light mineral oil, deionized water, and ethyl alcohol using the TeachSpin PS2 NMR Spectrometer. We characterized the transverse relaxation times T_2^* and T_2 and the longitudinal relaxation time T_1 for each sample, highlighting their molecular interactions and field effects.

The measured T_1 and T_2 times exhibit trends reflective of molecular structure and dynamics: deionized water with weaker molecular interactions (hydrogen bonds), displayed the longest relaxation times, while light mineral oil, with higher viscosity and stronger molecular interactions (covalent bonds), exhibited the shortest. T_2^* was uniformly short across all samples, primarily influenced by magnetic field inhomogeneities. Comparison of T_2 values obtained using different methods (Meiboom-Gill multipulse sequence versus one single two-pulse spin-echo) revealed the significant influence of frequency drift on relaxation measurements.

We also quantified magnetic field inhomogeneities ΔB_0 and frequency drift over time, observing their consistency with theoretical expectations. To mitigate drift, we recommend allowing the system to equilibrate for approximately 20 minutes prior to measurements.

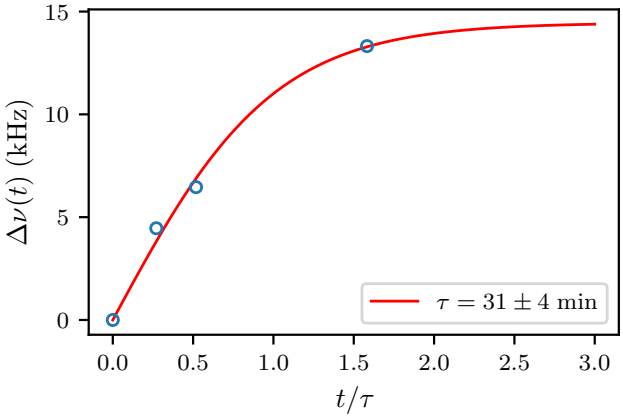

(a) Mineral Oil October 17, 2024

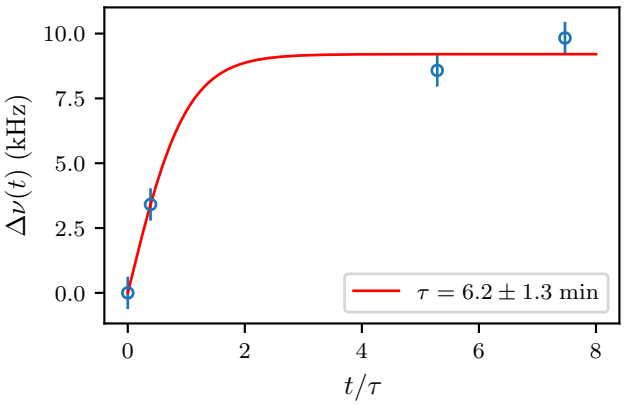

(b) Ethyl Alcohol November 14, 2024

FIG. 10: Frequency drift.

This study successfully demonstrates the application of NMR techniques for material characterization and underscores the sensitivity of relaxation times to both sample properties and experimental conditions. The findings align with theoretical models and provide robust framework for future NMR analyses using the TeachSpin apparatus.

[1] C. Cohen-Tannoudji, B. Diu, and F. Laloë, *Quantum Mechanics, Volume 1: Basic Concepts, Tools, and Applications* (Wiley, 2019).